sciendo

Investigation of Cu(In, Ga)Se2 solar cell performance with non-cadmium buffer layer using TCAD-SILVACO

BECHLAGHEM SARA*, ZEBENTOUT BAYA, BENAMARA ZINEB

Applied Microelectronic Laboratory, Faculty of Electrical Engineering,
Djillali Liabes University of Sidi Bel Abbes, 22000, Algeria

The purpose of this work is to achieve the best efficiency of Cu(In, Ga)Se2 solar cells by replacing the CdS buffer layer with other nontoxic materials. The simulation tool used in this study is Silvaco-Atlas package based on digital resolution 2D transport equations governing the conduction mechanisms in semiconductor devices. The J-V characteristics are simulated under AM1.5G illumination. Firstly, we will report the modeling and simulation results of CdS/CIGS solar cell, in comparison with the previously reported experimental results [1]. Secondly, the photovoltaic parameters will be calculated with CdS buffer layer and without any buffer layer to understand its impact on the output parameters of solar cells. The simulation is carried out with the use of electrical and optical parameters chosen judiciously for different buffers (CdS, ZnOS and ZnSe). In comparison to simulated CdS/CIGS, the best photovoltaic parameters have been obtained with ZnOS buffer layer. The structure has almost the same open circuit voltage Voc and fill factor FF, and higher short circuit current density Jsc, which results in slightly higher conversion efficiencies.

Keywords: *CIGS; ZnS; ZnOS; ZnSe; Atlas-SILVACO*

1. Introduction

In today's solar power industry, about 90 % of solar panels are made from silicon materials. However, the high cost of crystalline silicon, which accounts for nearly 50 % of the Module, pushed the manufacturers to look for other materials less expensive, to produce the solar cells. Among those materials, two options stand out in recent years due to their performance and simplicity for implementing: the die of CdTe and CuInSe2 (and its variant Cu(In, Ga)Se2 still called CIGS), both often associated with the CdS buffer layer [2].

The solar cells based on CIGS, consisting of a stack of layers contain a thin layer called the buffer layer between the absorber and the window layers. One of the most important benefits of this thin layer is protecting the CIGS interface during the deposition of the window layer. A buffer material should be n-type to make a junction with a p-CIGS absorber [3].

Conversion efficiencies exceeding 19 % for thin-film solar cells based on CIGS cells with CdS buffer layers prepared by the chemical bath deposition CBD method have been reported by several groups over the past few years [4, 5]. However, the toxicity of cadmium forces the research community to replace CdS buffer layer by other alternative, while preserving already achieved performance. In different laboratories, the films based on ZnOS [6–8], ZnSe [9–11], (Zn,Mg)O [12], In(OH) [13], were deposited on differently processed absorbers and tested as an alternative to the traditional CdS buffer. The ZnOS and ZnSe buffer layers are one of the most favorable candidates for replacing the CdS because both ZnOS and ZnSe possess large optical gaps.

2. Atlas numerical model description

In this work, The CIGS solar cells are modeled using Atlas-2D simulator. This is a software package from SILVACO [14] that is a physically-based two- and three-dimensional device simulator.

---

*E-mail: sar22000@yahoo.com

It predicts the device electrical behavior and enables the design of microelectronic devices for obtaining terminal characteristics (I-V, C-V...). This numerical program is capable of solving the basic semiconductor transport equations and consequently can be adapted to simulate thin film solar cells. The numerical method mainly used in Atlas to solving the basic semiconductor equations is the coupled Newton method which corresponds to an iterative resolution of a system regrouping three differential equations. The basic equations are: the Poisson equation 1, the continuity equations for electrons, equation 2 and holes, equation 3. They are mathematically described by the following relations:

Poisson equation:

$$\varepsilon \, \Delta V = - \, q \, \left(p - n + N_D^+ + N_A^- + N_T \right) \quad (1)$$

Continuity equations:

$$\frac{\partial n}{\partial t} = G_n - R_n + \frac{1}{q} div \, \vec{J}n \quad (2)$$

$$\frac{\partial p}{\partial t} = G_p - R_p + \frac{1}{q} div \, \vec{J}p \quad (3)$$

with $\vec{J}n$ and $\vec{J}p$ explained by the drift-diffusion model:

$$\vec{J}n = qn \, \mu_n \vec{E} + qD_n \, \vec{grad} \, n \quad (4)$$

$$\vec{J}p = qp \, \mu_p \vec{E} + qD_p \, \vec{grad} \, p \quad (5)$$

where V is the electrostatic potential, ϵ is the permittivity, q is the charge of an electron, n free electron concentration, p free hole concentration, N_D^+ the ionized donor-like doping concentration and N_A^- the ionized acceptor-like doping concentration, N_T describes the presence of some defect centers or traps (donor-type or acceptor-type) in the semiconductor bulk or at the interfaces, which can significantly affect the electrical characteristics of the device. Jn and Jp are the electron and hole current densities, Gn(Rn) and Gp(Rp) are the generation (recombination) rates for the electrons and holes, respectively. E is the electric field, μn and μp are the electron and hole mobilities, Dn and Dp are the electron and hole diffusion constants.

3. Solar cell structure and materials parameters

At first, CIGS solar cell with CdS buffer layer was simulated. The device properties (physical, electrical and optical) were reported in Table 1 from experimental CIGS solar cells [1].

The simulated CdS/CIGS solar cell structure is shown in Fig. 1. It is formed by a p-type CIGS absorber and n-type CdS (buffer). A transparent contact of ZnO layer is deposited on the top of the structure while the Mo (molybdenium) is deposited on the back.

This solar cell was illuminated under AM 1.5G solar spectrum with 100 mW·cm^{-2} incident power density. The set parameters of each layer are indicated in Table 1.
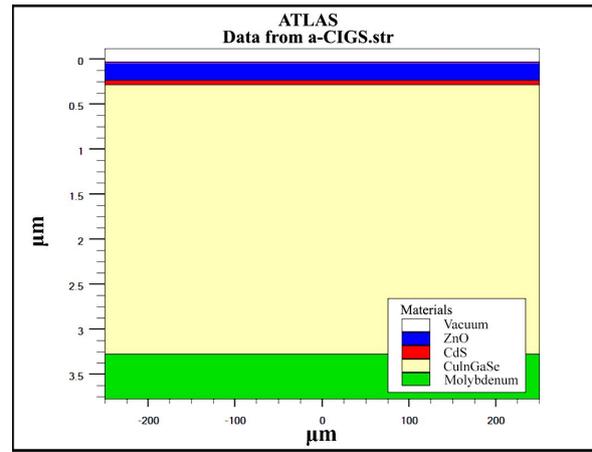
Fig. 1. Control CdS/CIGS solar cell used for a baseline simulation.

The concentration of the majority carriers in the CIGS have been studied by different research groups. The values around 10^{16} cm^{-3} were given in the literature [15]. The differences of affinity (CBO or ΔEc: conduction band offset) between the absorber and different buffers were estimated based on previous measurements by Bjorkman et al. [16, 17]. The optimal condition for CBO between the buffers and CIGS is a small positive offset [15, 17–19], while the negative CBO between the buffers and the ZnO window was taken from Gloeckler et al. [15] and Bjorkman et al. [16].

Table 1. Materials parameters used in the simulation.

Layer properties	ZnO	CdS	CIGS	ZnOS	ZnSe
Thickness [nm]	200	500	3000	500	500
Band gap energy [eV]	3.3	2.48	1.17	2.97/2.65	2.58
Dielectric constant	9	10	13.6	8.3	8.1
Carrier concentration [cm^{-3}]	D:5×10^{17}	D:2×10^{18}	A:8×10^{16}	D:2×10^{18}	D:2×10^{18}
Electron mobility μ_n[cm^2/Vs]	100	100	100	100	100
Hole mobility μ_p [cm^2/Vs]	25	25	25	25	25
Conduction band effective density of states N_C [cm^{-3}]	2.2×10^{18}	2.2×10^{18}	2.2×10^{18}	2.2×10^{18}	2.2×10^{18}
Valence band effective density of states N_V [cm^{-3}]	1.8×10^{19}	1.8×10^{19}	1.8×10^{19}	1.8×10^{19}	1.8×10^{19}
Conduction band offset [eV]	-0.2	$+0.4$	$-0.2/0$	$-0.2/0$	
Gaussian-distributed defect states					
Bulk defect concentration	D:10^{17}	A:10^{16}	D:10^{14}	A:10^{16}	A:10^{16}
Standard deviation Wg [eV]	0.1	0.1	0.1	0.1	0.1
Capture cross section for electrons and holes [cm^2]	$10^{-12}/10^{-15}$	$10^{-16}/10^{-12}$	$2 \times 10^{-13}/10^{-15}$	$10^{-16}/10^{-12}$	$10^{-16}/10^{-12}$

The band gaps of ZnO, CdS and ZnSe were taken from the Silvaco database. Whereas an approximate expression 6 of the band gaps of the Cu In$_{(1-x)}$Ga$_x$Se alloys was used from [20], with x being Ga anion fraction:

$$Eg(x) = 1.01 + 0.42\,x + 0.24\,x^2 \qquad (6)$$

The band gap of CIGS ranges from 1.01 eV to 1.67 eV but currently the best CIGS based solar cells have a Ga content of 0.3 to 0.4 [21, 22], which corresponds to Eg of 1.1 eV to 1.2 eV and in our study we chose x = 0.3 giving Eg = 1.17 eV. Another approximate expression 7 for the band gaps of the ZnOS alloys was used from the literature [20] with Z being the oxygen ratio:

$$Eg(Z) = 3.6 - 0.4Z - 3Z(1 - Z) \qquad (7)$$

The band gap of ZnOS ranges from 2.64 eV to 3.6 eV depending on the value of the oxygen /sulfur ratio [20]. In this study, we chose Z = 0.9 in section 4.2 of this paper which corresponds to the band gap energy of 2.97 eV and CBO = 0 eV. In addition, we chose Z = 0.5 in section 4.3 to get an optimal CBO of 0.4 eV as investigated by Gloeckler et al. [23] corresponding to a band gap energy of 2.65 eV.

The electron mobility μn, the hole mobility μp, the conduction band effective density of states N_C and the valance band effective density of states Nv of each material were set according to the literature [15, 24, 25].

The optical parameters of ZnO and ZnS and CIGS are based on Zeman et al. [26], Debenham [27] and Paulson et al. [28], respectively. The parameters for ZnSe and CdS were taken from Silvaco database, while for metal contact layer (Mo) they were available in SOPRA database of the Atlas software. Reflection losses from the surface of the solar cell were also integrated into the model. In this study, the solar cells operating temperature was set at 300 K.

We have a large number of defects in this simulation because all the layers are polycrystalline. In our simulation we have a Gaussian deep donor defect for the CIGS, a Gaussian deep acceptor defect for the different buffers and Gaussian deep donor defect for the ZnO. Interface recombination velocity of electrons and holes were chosen equal to 10^7 cm/s at the semiconductor hetero-interfaces (buffer/CIGS) and at the front and back contacts.

After adjusting all the necessary parameters as shown in Table 1, our simulation results were compared with the experimental data by Jackson et al. [1] in Table 2. We can conclude that the results of our simulation are in a good agreement with the experiments and validate our parameters used in the simulation.

Table 2. Simulated and experimental output parameters of a CIGS based solar cell.

	Jsc [mA/cm^2]	Voc [V]	FF [%]	η [%]
Silvaco	36.4	0.680	80.22	19.88
Literature	36.3	0.740	77.5	20.3

4. Results and discussion

4.1. The role of the buffer layer in CIGS based solar cells

Solar cell performances as a function of the CIGS solar cell with and without any buffer layer are shown in Table 3, while the corresponding J-V characteristics are shown in Fig. 2.

Table 3. Performance of simulated CIGS based solar cell with and without buffer layer.

	Jsc [mA/cm^2]	Voc [V]	FF [%]	η [%]
with CdS	36.4	0.680	80.22	19.88
without CdS	34.8	0.478	71.09	11.85

As it can be seen in Table 3 and Fig. 2, there is a decrease in all photovoltaic parameters, when we simulate directly ZnO/CIGS solar cell. We must point out that simulated devices having ZnO directly on the CIGS layer are characterized by poor photovoltaic characteristics. Typically, much lower voltages and fill factors are observed in comparison to the devices with CdS buffer layer because one of the critical elements of CIGS based solar cells is the p-n junction formation. The preferred approach is the deposition of a thin CdS layer, according to Ramanathan et al. [29].
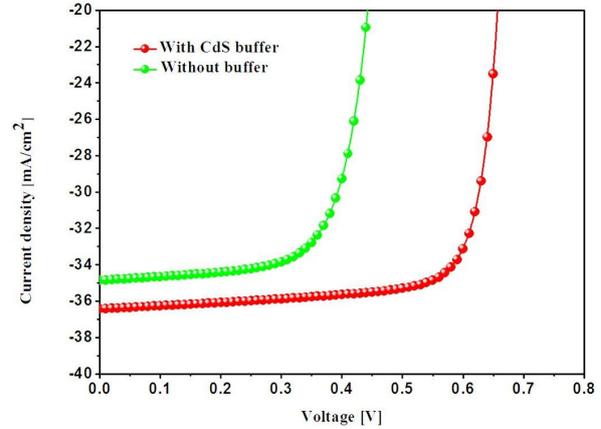
Fig. 2. J-V curves of CIGS based solar cells with and without buffer layer.

4.2. Alternative buffer layer

The second goal in this study was to explore the benefits of using the wide-gap ZnOS and ZnSe buffers in place of the traditional 2.4 eV CdS. The solar-cell performance parameters Jsc, Voc, FF, and η are shown in Table 4 (column A) and the corresponding J-V characteristics are illustrated in Fig. 3; they are shown for different buffer layers: CdS, ZnOS and ZnSe.

Table 4. Performance of simulated CIGS based solar cells with different buffer layers.

	CdS	A ZnOS (CBO = 0)	ZnSe	B ZnOS (CBO = 0.4)
Jsc [mA/cm^2]	36.4	37.4	35.5	37.7
Voc [V]	0.680	0.624	0.622	0.680
FF [%]	80.22	79.20	78.79	80.42
η [%]	19.88	18.53	17.46	20.63

Concerning Table 4 (column A), it may be noted that solar cell with CdS layer has the best conversion efficiency. But it is clear from Fig. 3 that the use of higher band gap Zn (O, S) compared to CdS, results in higher short circuit current, allowing for enhanced collection of short-wavelength photons as published in other papers [30]. Thus, we suggest that we can achieve good performances with other buffer layer made of nontoxic elements.
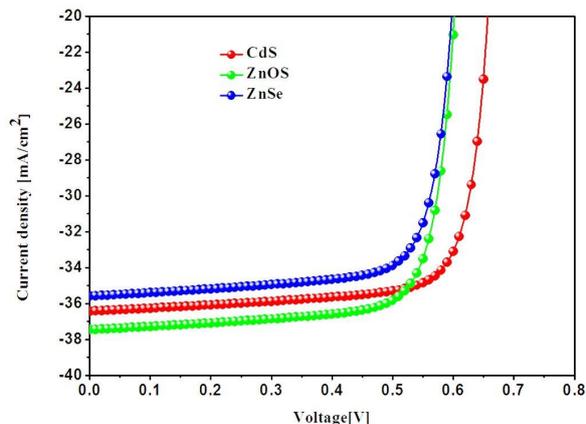
Fig. 3. Illuminated J-V curves of CIGS based solar cell with different buffer layers.

4.3. Effect of CBO on ZnOS/CIGS solar cells

The solar cell performance parameters Jsc, Voc, FF, and η for ZnOS /CIGS based solar cell with CBO = 0.4 eV are shown in Table 4 (column B), whereas the J-V characteristics for the solar cells with different buffer layers are shown in Fig. 4.
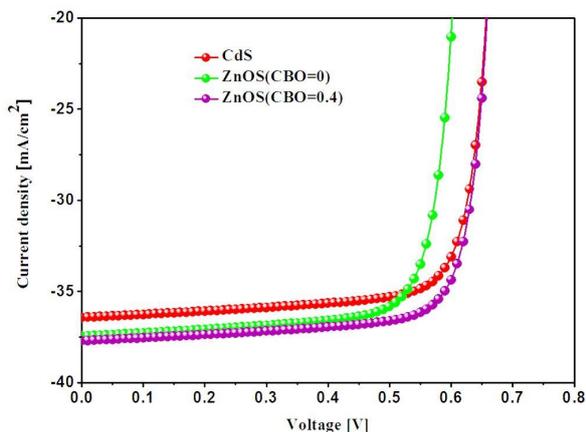
Fig. 4. Effect of the conduction band offset on J-V characteristics of ZnOS/CIGS structure.

For ZnOS, the CBO should increase with sulfur and oxygen content according to theoretical studies [31]. Table 4 (column B) shows that the ZnOS/CIGS based solar cell with a slightly larger positive CBO = +0.4 eV shows an enhancement in open circuit voltage Voc (0.680 V), fill factor FF (about 80.42 %) and efficiency η (20.63 %), as well

as a slight improvement in short circuit current Jsc (about 37.7 mA/cm^2), compared to the same structure (ZnOS/CIGS) with CBO = 0.

The short circuit current density of ZnOS/CIGS structure with CBO = +0.4 eV compared to the CdS/CIGS structure shows an increment of about 1.3 mA/cm^2, and also the efficiency is somewhat higher, which is clearly illustrated in Table 4 and Fig. 4, because the higher band-gap of ZnOS of about 2.65 eV enhances the collection of short-wavelength photons.

From these results it can be concluded that a performance comparable to the simulated solar cells with CdS buffer layer can be achieved and even exceed them, which is in a good agreement with Nakada et al. [32]. The above results imply that a favorable band alignment is necessary to achieve high performance, that is to say an optimal CBO of about +0.4 eV between buffers and CIGS.

5. Conclusions

In this study, we have investigated optical and electrical properties of CIGS based solar cells with non-cadmium buffer layer using Atlas-SILVACO tools. It is found that the CIGS based solar cells with ZnOS buffer layer are suitable as Cd-free candidate for buffer layers. The device efficiency as well as short current density Jsc are improved.

The major advantage of these alternative buffers is that their bandgap is larger than the band gap of CdS. It is worth noting that the ZnOS present a wide range of energy bandgaps from 2.64 eV to 3.6 eV achieved through modification of oxygen-to-sulfur ratio [20] which allows for enhanced collection of high energy photons which should increase current density. The optimal condition is a small positive offset between buffers and CIGS. Gloeckler et al. [23] showed that the range of an optimal band alignment is approximately from +0.1 eV to +0.4 eV.

This study explored the use of other materials, especially ZnOS, as an alternative buffer layer to CdS because it offers higher photocurrent. Another

advantage of replacing CdS is that elimination of cadmium reduces the overall toxicity of the resulting cell which is a relevant issue for the industry.

References

[1] JACKSON P., HARISKOS D., LOTTER E., PAETEL S., WUERZ R., MENNER R., WISCHMANN W., POWALLA M., *Prog. Photovoltaics*, 19 (2011), 894.

[2] JEFFERY L.G., RICHARD J.S., LEE Y.J., *Numerrical modeling of CIS and CDTE solar cells*, ECE-Technical Reports, Indiana, 1994.

[3] HARISKOS D., SPIERING S., POWALLA M., *Thin Solid Films*, 48 (2005), 99.

[4] RAMANATHAN K., CONTRERAS M.A., PERKINS C.L., ASHER S., HASOON F.S., KEANE J., YOUNG D., ROMERO M., METZGER W., NOUFI R., WARD J., DUDA A., *Prog. Photovoltaics*, 11 (2003), 225.

[5] CONTRERAS M.A., RAMANATHAN K., ABUSHAMA J., HASOON F., YOUNG D.L., EGAAS B., NOUFI R., *Prog. Photovoltaics*, 13 (2005), 209.

[6] CONTRERAS M.A., NAKADA T., HONGO M., PUDOV A.O., SITES J.R., *Proceedings 3rd World Conference of Photovoltaic Energy Conversion*, Osaka, 2003, p. 570.

[7] BJORKMAN C.P., KESSLER J., STOLT L., *Proceedings 3rd World Conference of Photovoltaic Energy Conversion*, Osaka, 2003, p. 461.

[8] MUFFLER H.J., BAER M., FISCHER C.H., GAY R., KARG F., LUX-STEINER M.C., *Proceedings 28th IEEE Photovoltaic Specialist Conference, Anchorage*, Alaska, 2000, p. 610.

[9] ENNAOUI A., SIEBENTRITT S., LUX-STEINER M.C., RIEDL W., KARG F., *Sol. Energ. Mat. Sol. C.*, 67 (2001), 31.

[10] EISELE W., ENNAOUI A., SCHUBERT-BISCHOFF P., GIERSIG M., PETTENKOFER C., KRAUSER J., LUX-STEINER M.C., ZWEIGART S., KARG F., *Sol. Energ. Mat. Sol. C.*, 75 (2003), 17.

[11] MUNZEL M., DEIBEL C., DYAKONOV V., PARISI J., RIEDL W., KARG F., *Thin Solid Films*, 387 (2001), 231.

[12] NEGAMI T., AOYAGI T., SATOH T., SHIMAKAWA S., HAYASHI S., HASHIMOTO Y., *Proceedings 29th IEEE Photovoltaic Specialist Conference*, New Orleans, 2002, p. 656.

[13] TOKITA Y., CHAISITSAK S., MIYAZAKI H., MIKAMI R., YAMADA A., KONAGAI M., *Jpn. J. Appl. Phys.*, 41 (2002), 7407.

[14] SILVACO, INC, *Atlas User's Manual*, Santa Clara, CA, 2013.

[15] GLOECKLER M., SITES J.R., METZGER W.K., *J. Appl. Phys.*, 98 (2005), 113704.

[16] BJORKMAN C.P., TORNDAHL T., ABOU-RAS D., MALMSTRÖM J., KESSLER J., STOLT L., *J. Appl. Phys.*, 100 (2006), 044506.

[17] BJORKMAN C.P., LU J., KESSLER J., STOLT L., *Thin Solid Films*, 431 (2003), 321.

[18] PUDOV A.O., CONTRERAS M.A., NAKADA T., SCHOCK H.W., SITES J.R., *Thin Solid Films*, 480 (2005), 273.

[19] PUDOV A.O., HASOON F.S., KANEVCE A., AL-THANI H., SITES J.R., *J. Appl. Phys.*, 6 (2005), 4901.

[20] SHARBATI S., SITES J.R., *IEEE J. Photovolt.*, 4 (2014), 2.

[21] REPINS I., CONTRERAS M.A., EGAAS B., DEHART C., SCHARF J., PERKINS C.L., TO B., NOUFI R., *Prog. Photovoltaics*, 16 (2008), 235.

[22] POWALLA M., VOORWINDEN G., HARISKOS D., JACKSON P., KNIESE R., *Thin Solid Films*, 517 (2009), 2111.

[23] GLOECKLER M., SITES J.R., *Thin Solid Films*, 480 (2005), 241.

[24] CHELVANATHAN P., HOSSAIN M., AMIN N., *Curr. Appl. Phys.*, 10 (2010), 387.

[25] SHARBATI S., KESHMIRI S.H., MCGOFFIN J.T., GEISTHARDT R., *Appl. Phys. A-Mater.*, 4 (2015), 1259.

[26] ZEMAN M., SWAAIJ R., METSELAAR J., *J. Appl. Phys.*, 88 (2000), 6436.

[27] DEBENHAM M., *Appl. Optics*, 23 (1984), 2238.

[28] PAULSON P.D., BIRKMIRE R.W., SHAFARMAN W.N., *J. Appl. Phys.*, 94 (2003), 879.

[29] RAMANATHAN K., WIESNER H., ASHER S., NILES D., BHATTACHARYA R.N., CONTRERAS M.A., NOUFI R., *2nd World Conference and Exhibition on Photovoltaic Solar Energy Conversion*, Vienna, July, 6 – 10, 1998.

[30] PUDOV A.O., SITES J.R., NAKADA T., *Jpn. J. Appl. Phys.*, 41 (2002), 672.

[31] SU-HUAI W., ZUNGER A., *Appl. Phys. Lett.*, 72 (1998), 2011.

[32] NAKADA T., MIZUTANI M., HAGIWARA Y., KUNIOKA A., *Sol. Energ. Mat. Sol. C.*, 67 (2001), 255.